

## 19. DATA REPORT: SPECTRAL REFLECTANCE OBSERVATIONS FROM RECOVERED SEDIMENTS<sup>1</sup>

Joseph D. Ortiz,<sup>2</sup> Suzanne O'Connell,<sup>3</sup> and Alan Mix<sup>4</sup>

### ABSTRACT

Sediment spectral reflectance measurements were generated aboard the *JOIDES Resolution* during Ocean Drilling Program Leg 162 shipboard operations. The large size of the raw data set (over 1.3 gigabytes) and limited computer hard disk storage space precluded detailed analysis of the data at sea, although broad band averages were used as aids in developing splices and determining lithologic boundaries. This data report describes the methods used to collect these data and their shipboard and postcruise processing. These initial results provide the basis for further postcruise research.

### INTRODUCTION

Spectral reflectance provides a rapid, high-resolution, noninvasive tool for characterization of downcore mineralogical variations in deep-sea sediments. This can be demonstrated by comparison of the percent reflectance data with shipboard carbonate measurements (fig. 9, Shipboard Scientific Party, 1996b). On board the *JOIDES Resolution*, sediment reflectance measurements were used as an aid in identifying lithologic unit boundaries and for assistance in developing composite, spliced records at each site. Reflectance provided the primary criteria for splice determination at Site 982, which lacked a strong lithogenic signal. The processed reflectance data described in this report are included on the Ocean Drilling Program (ODP) Leg 162 *Scientific Results* volume CD-ROM (see back pocket, this volume) for scientific use.

### METHODS

Sediment reflectance was measured at sea during Leg 162 using the Oregon State University (OSU) split-core analysis track (SCAT). Measurements were conducted by the shipboard sedimentologists on the lightly scraped archive half of wet sediment cores during the core description process. Sections were not wrapped in plastic (e.g., Glad-wrap) during measurement. Plastic wrapping is recommended for use with the shipboard, handheld Minolta CM-2002 spectrophotometer to protect its integrating sphere and/or the glass lens of its granular materials cover set from direct contact with sediments (Shipboard Scientific Party, 1995; Balsam et al., 1997). However, plastic wrapping of sections before reflectance measurement with the SCAT would interfere with its conductivity landing system. It is thus unnecessary because the sample port of the SCAT's integrating sphere is designed not to touch the sediments. The Leg 162 configuration of the SCAT was first used during postcruise operations during ODP Leg 154 (Harris et al., 1997). Reflectance measurements with this version of the instrument have a signal-to-noise ratio that is an order of magnitude better than the prototype instrument deployed during Leg 138 (Harris et al., 1997; Mix et al., 1992, 1995).

The SCAT system consists of a computer-controlled, motorized, horizontal track assembly that advances a core section into measurement position under a light-integrating sphere (Fig. 1). The integrating sphere is lowered, and the conductivity and/or strain sensors are brought into contact with the sediment using a computer-controlled, vertical stepping motor. Measurements are conducted on a 2-cm spot size. Temperature, conductivity, and strain sensors determine contact with the sediment and gently land the sensor head on the sediments for measurement. Light of known spectral properties from two light sources—one for visible and infrared wavelengths and a second for UV wavelengths—is supplied to the integrating sphere via fiber optics and directed by a beam-steering mirror. Each measurement cycle consists of an internal black background measurement (with no light input), an internal white calibration measurement of a Spectralon reference target, and the sample measurement. These internal calibration measurements allow instrument counts to be converted to raw percent reflectance.

In addition, external calibration measurements are conducted to ensure that there are no section-to-section offsets and to correct for scattering errors associated with the integrating sphere (Fig. 1). This step is necessary because real-world integrating spheres are not ideal reflectors (Clarke and Compton, 1986). The raw percent reflectance measurements are corrected using external Spectralon standards with known reflectance of 2%, 40%, 75%, and 100% that were measured approximately every 7 to 14 sections (10–20 m) to ensure the highest quality data.

The light that is diffusely reflected off the sediments is integrated within the sphere and then divided into its constituent wavelengths by a diffraction grating and collected with a multichannel detector. This detector measures 1024 wavelength bands (0.68 nm wide) ranging from 250 to 950 nm (UV to nIR). These measurements were generally taken at 8-cm intervals, although higher resolution (4-cm interval) measurements were taken when time permitted. All cores (advanced hydraulic piston corer and some extended core barrel) from a designated hole (usually the "A" hole) were scanned at each site. To ensure that composite reflectance splices could be generated, cores from additional holes at each site (guided by comparison to multisensor track data) were selected for analysis. Because of time constraints, the upper sections of Site 981 (~0–90 mcd) were not analyzed: this sediment sequence represents a lower sedimentation rate repeat of the upper sediment sequence at Site 980 (Shipboard Scientific Party, 1996a).

### DATA

A total of 55,159 reflectance measurements were generated during the shipboard operations of Leg 162. These measurements were

<sup>1</sup>Raymo, M.E., Jansen, E., Blum, P., and Herbert, T.D. (Eds.), 1999. *Proc. ODP, Sci. Results*, 162: College Station, TX (Ocean Drilling Program).

<sup>2</sup>Lamont-Doherty Earth Observatory of Columbia University, Rt. 9W, Palisades, NY 10964, U.S.A. jortiz@ldeo.columbia.edu

<sup>3</sup>Department of Earth and Environmental Sciences, 265 Church St., Wesleyan University, Middletown, CT 06459, U.S.A.

<sup>4</sup>College of Oceanic and Atmospheric Sciences, 104 Ocean Administration Building, Corvallis, OR 97330-5503, U.S.A.

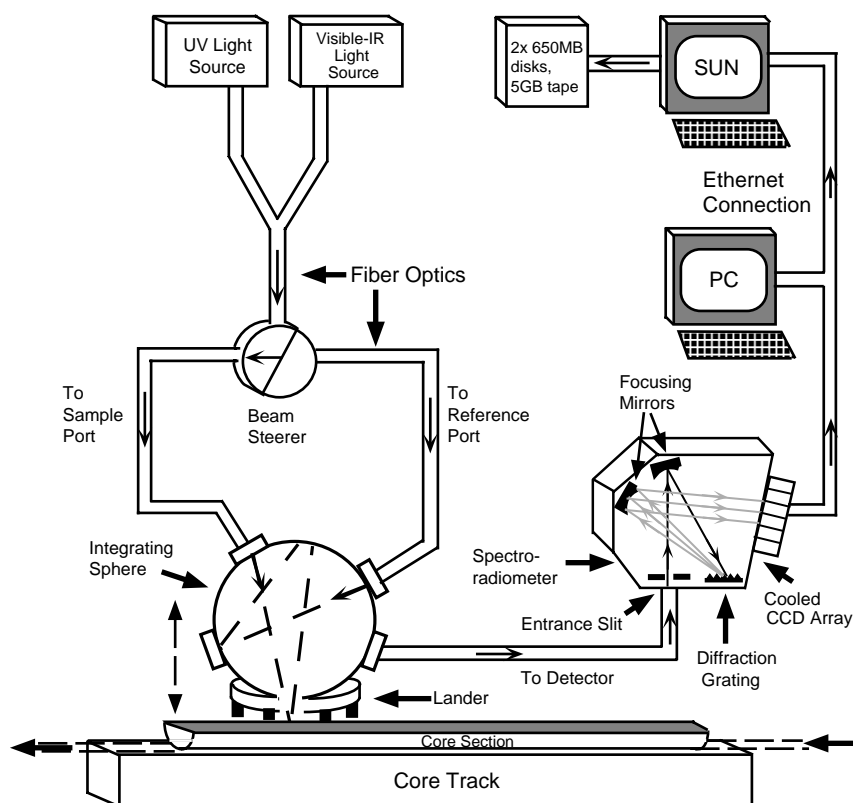


Figure 1. A schematic illustrating the various components of the OSU SCAT system. (Drawing not to scale.)

produced for one or more holes at all of the sites that were drilled during this leg. Summary statistics of these data are provided in Table 1. Processed data from all of these sites are available in a number of forms. For shipboard analysis, percent reflectance was averaged into four 50-nm-wide bands defined as UV (250–300 nm), blue (450–500 nm), red (650–700 nm), and nIR (900–950 nm). These data can be found in the TABLE\_2 directory on the volume CD-ROM (back pocket, this volume). During shipboard operations, blue band percent reflectance values were compared with the closest available carbonate measurements to determine if there was a consistent relationship between sediment carbonate content and reflectance (Fig. 2).

Postcruise analysis consisted in part of quality control to assure that there were no measurement offsets and of averaging the high-resolution data into a 10-nm resolution percent reflectance data set. These data can be found in the TABLE\_3 directory on the volume CD-ROM (back pocket, this volume). The 10-nm resolution data were used in conjunction with shipboard percent  $\text{CaCO}_3$  data to develop proxy percent  $\text{CaCO}_3$  records. Examples of downcore reflectance variations at the 10-nm wavelength band centered on 665 nm for Sites 980–984 are plotted in Figure 3. This band is selected for illustration because it is close to the maximum output response of the instrument.

The first derivative of the reflectance spectra (i.e., its “spectral shape”) is useful for assessment of sediment mineralogy (Balsam and Deaton, 1991; Deaton and Balsam, 1991). The 10-nm resolution data were used to calculate center-weighted, first-derivative spectra (see the TABLE\_4 directory on the volume CD-ROM [back pocket, this volume]). We use centered-weighted first derivatives (calculated based on data from above and below the central wavelength) rather than simple first-difference derivatives (calculated between two reflectance measurements) because they are numerically more stable (Press et al., 1992). Examples of downcore variations of the first derivative at 565 nm for Sites 980–984 are plotted in Figure 4. Increases in the first derivative at this wavelength are related to increases in sediment hematite concentration (Deaton and Balsam, 1991). The average reflectance spectra for Sites 980–984 (Fig. 5) exhibit peaks for

Table 1. Statistics on the reflectance observations collected during Leg 162.

Hole	Mean percent red reflectance (600–650 nm)	S.D. percent red reflectance (600–650 nm)	Number of observations
162-			
980A	20.23	9.59	2087
980B	20.25	9.78	1526
980C	17.63	9.26	1221
981A	35.33	10.51	2997
981B	30.98	8.63	878
981C	31.91	9.74	688
982A	54.41	14.36	2044
982B	56.44	13.39	3526
982C	55.11	15.64	1160
982D	29.80	12.90	57
983A	8.39	2.77	3128
983B	7.65	2.93	3402
983C	7.58	2.74	3242
984A	7.34	2.09	1822
984B	6.51	2.29	3459
984C	6.51	2.27	3191
984D	7.60	2.42	170
907B	9.37	3.94	3217
907C	8.41	2.54	3093
985A	9.78	3.07	3292
985B	10.80	3.80	1567
986A	7.60	2.06	1631
986B	10.54	2.41	168
986C	7.54	2.00	1707
987A	8.75	1.98	1930
987B	8.95	2.64	755
987C	10.66	2.98	516
987D	8.54	1.98	2450

Note: S.D. = standard deviation.

smectite, chlorite, hematite, and a broad absorption band. The latter is associated with organic carbon absorption based on comparison with the factors described in Deaton and Balsam (1991).

For ease of comparison, the reflectance data in Figures 3 and 4 have been plotted vs. age (Ma), based on biostratigraphic and magnetostratigraphic age constraints determined during Leg 162. With the

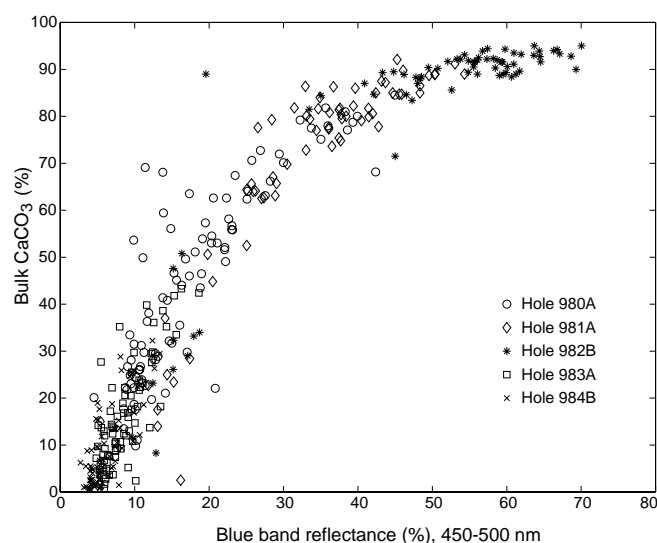


Figure 2. Spectral reflectance (450–500 nm) in relation to the bulk calcium carbonate content of sediments recovered from Leg 162, Sites 980 through 984. Open circles = Hole 980A, open diamonds = Hole 981A, stars = Hole 982B, open squares = Hole 983A, × symbols = Hole 984B. (Fig. 9, Shipboard Scientific Party, 1996b.)

exception of the age model for Site 980, these age models are presented in the sedimentation rate sections of the Leg 162 *Initial Reports* volume (Jansen, Raymo, Blum, et al., 1996). To match the records for Sites 980 and 981 between 1.5 and 1.7 Ma, we visually correlated the Site 980 record with that of Site 981, which has better age control for this time interval (Table 5). The Site 981 age model used here employs the deeper pick (179.48 mcd) for the Matuyama/Gauss boundary (Shipboard Scientific Party, 1996a).

## SUMMARY OF RESULTS

Focusing on the North Atlantic drift sites during the past 2.5 m.y., the reflectance measurements yield consistent patterns from site to site that can be described as follows:

1. Percent reflectance at Sites 980 through 984 demonstrate a systematic relationship to sediment bulk calcium carbonate content (Fig. 2). Higher sediment reflectance (“brightness”) is associated with greater sediment bulk calcium carbonate content.
2. Sediments in the east (Sites 980/981 and 982) exhibit greater mean reflectance values and greater variations in percent reflectance than sediments from the west (Sites 983 and 984) (Table 1; Fig. 3).
3. Sediments older than 2.5 Ma exhibit systematically higher percent reflectance and lower variability than sediments younger than 2.5 Ma (Fig. 3).
4. At Sites 980/981 and 982, the first derivative of the reflectance spectra at 565 nm has low amplitude in sediments older than 2.5 Ma. The mean first derivative value at 565 nm at these sites increases with decreasing age.

5. Sites 983 and 984 exhibit much lower amplitude first-derivative variations at 565 nm than Sites 980/981 and 982.

## ACKNOWLEDGMENTS

We thank the captain and crew of the *JOIDES Resolution* and the co-chief scientists, M. Raymo and E. Jansen, for their assistance at sea. Sara Harris at Oregon State University has been an active collaborator. We also thank William Rugh, who provided much-needed assistance setting up the SCAT system on the *JOIDES Resolution*. This research was supported in part by a postcruise JOI/USSSP grant to JDO. This data report is LDEO contribution 5791.

## REFERENCES

- Balsam, W.L., Damuth, J.E., and Schneider, R.R., 1997. Comparison of shipboard vs. shore-based spectral data from Amazon-fan cores: implications for interpreting sediment composition. In Flood, R.D., Piper, D.J.W., Klaus, A., and Peterson, L.C. (Eds.), *Proc. ODP, Sci. Results*, 155: College Station, TX (Ocean Drilling Program), 193–215.
- Balsam, W.L., and Deaton, B.C., 1991. Sediment dispersal in the Atlantic Ocean: evaluation by visible light spectra. *Rev. Aquat. Sci.*, 4:411–447.
- Clarke, F.J.J., and Compton, J.A., 1986. Correction methods for integrating-sphere measurement of hemispherical reflectance. *Color Res. Appl.*, 11:253–262.
- Deaton, B.C., and Balsam, W.L., 1991. Visible spectroscopy: a rapid method for determining hematite and goethite concentrations in geological materials. *J. Sediment. Petrol.*, 61:628–632.
- Harris, S.E., Mix, A.C., and King, T., 1997. Biogenic and terrigenous sedimentation at Ceara Rise, western tropical Atlantic, supports Pliocene–Pleistocene deep-water linkage between hemispheres. In Shackleton, N.J., Curry, W.B., Richter, C., and Bralower, T.J., *Proc. ODP, Sci. Results*, 154: College Station, TX (Ocean Drilling Program), 331–345.
- Jansen, E., Raymo, M.E., Blum, P., et al., 1996. *Proc. ODP, Init. Repts.*, 162: College Station, TX (Ocean Drilling Program).
- Mix, A.C., Harris, S.E., and Janecek, T.R., 1995. Estimating lithology from nonintrusive reflectance spectra: Leg 138. In Pisias, N.G., Mayer, L.A., Janecek, T.R., Palmer-Julson, A., and van Andel, T.H. (Eds.), *Proc. ODP, Sci. Results*, 138: College Station, TX (Ocean Drilling Program), 413–427.
- Mix, A.C., Rugh, W., Pisias, N.G., Veirs, S., Leg 138 Shipboard Sedimentologists (Hagelberg, T., Hovan, S., Kemp, A., Leinen, M., Levitan, M., Ravelo, C.), and Leg 138 Scientific Party, 1992. Color reflectance spectroscopy: a tool for rapid characterization of deep-sea sediments. In Mayer, L., Pisias, N., Janecek, T., et al., *Proc. ODP, Init. Repts.*, 138 (Pt. 1): College Station, TX (Ocean Drilling Program), 67–77.
- Press, W.H., Teukolsky, S.A., Vetterling, W.T., and Flannery, B.P., 1992. *Numerical Recipes in Fortran: the Art of Scientific Computing*, (2nd ed.): New York (Cambridge Press), 180–184.
- Shipboard Scientific Party, 1995. Explanatory notes. In Curry, W.B., Shackleton, N.J., Richter, C., et al., *Proc. ODP, Init. Repts.*, 154: College Station, TX (Ocean Drilling Program), 11–38.
- Shipboard Scientific Party, 1996a. Sites 980/981. In Jansen, E., Raymo, M.E., Blum, P., et al., *Proc. ODP, Init. Repts.*, 162: College Station, TX (Ocean Drilling Program), 49–90.
- Shipboard Scientific Party, 1996b. Site 984. In Jansen, E., Raymo, M.E., Blum, P., et al., *Proc. ODP, Init. Repts.*, 162: College Station, TX (Ocean Drilling Program), 169–222.

Date of initial receipt: 25 August 1997

Date of acceptance: 11 June 1998

Ms 162SR-029

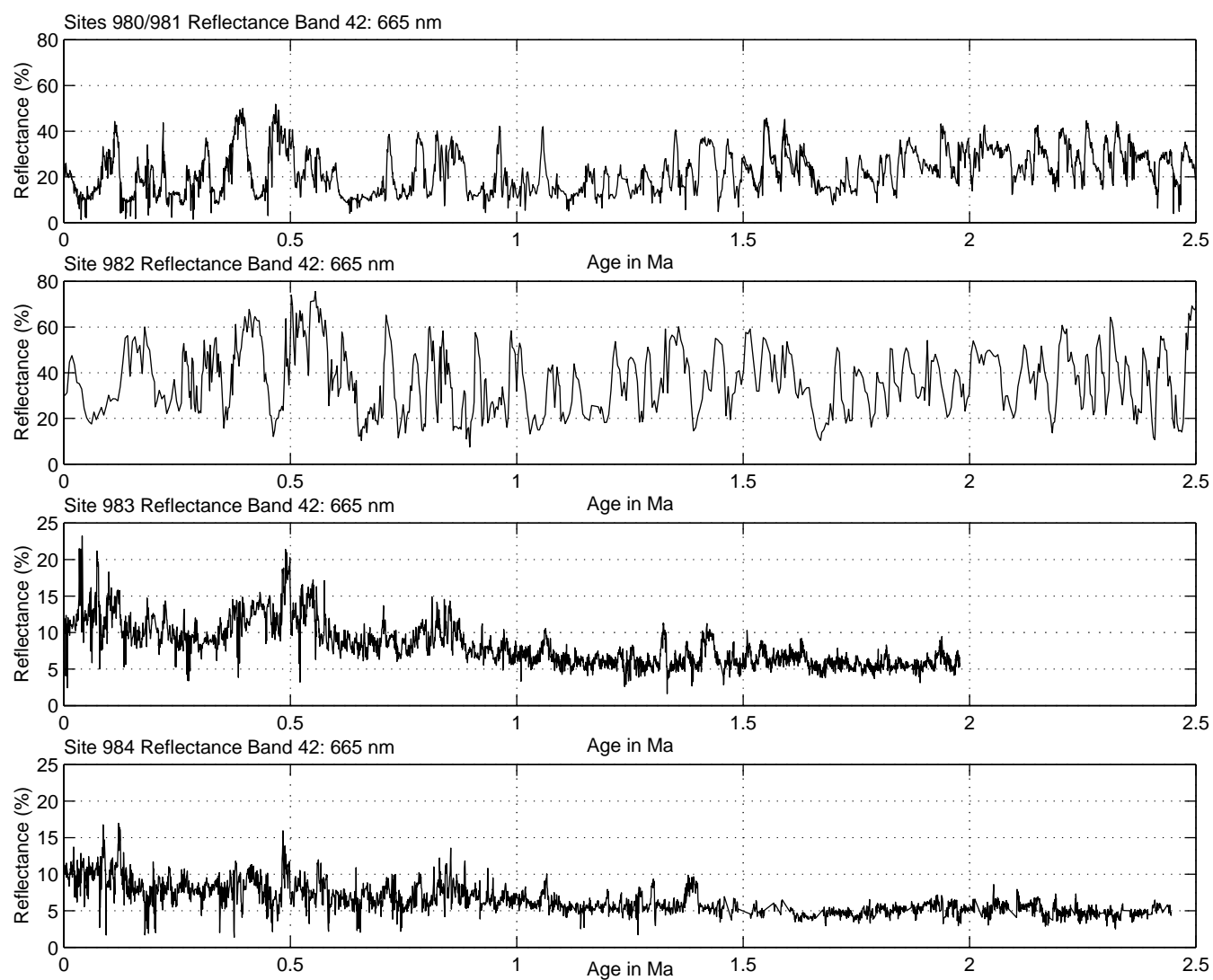


Figure 3. Downcore variations in diffuse spectral reflectance at 665 nm plotted against age (Ma) based on the shipboard age model for Sites 980 through 984.

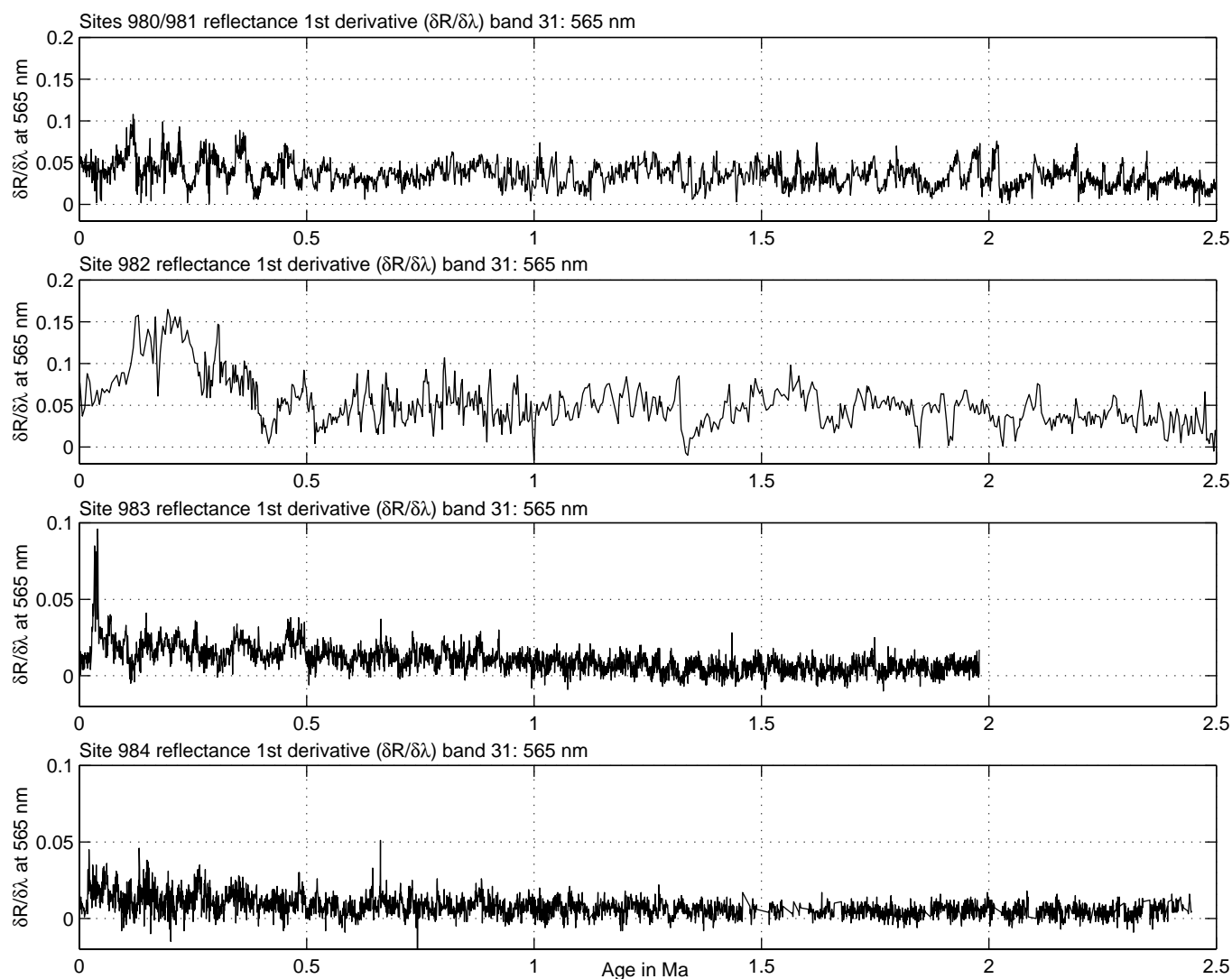


Figure 4. Downcore variations in the first derivative of diffuse spectral reflectance at 565 nm plotted against age (Ma) based on the shipboard age model for Sites 980 through 984.

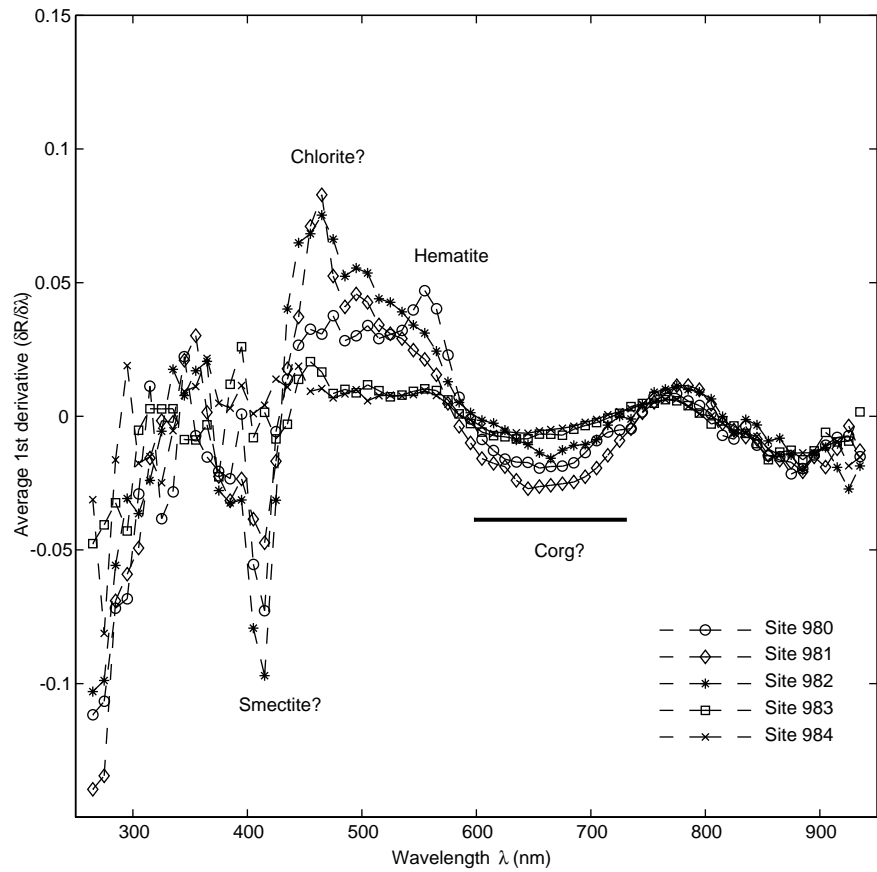


Figure 5. Average first-derivative spectra for Sites 980–984. Spectral peaks associated with various sediment components are identified based on comparison with the first-derivative factors of Balsam and Deaton (1991). Open circles = Site 980, open diamonds = Site 981, stars = Site 982, open squares = Site 983, × symbols = Site 984.

Table 5. Age model for Site 980.

Event	Depth (mcd)	Age (Ma)
Core top	0.00	0.000
FAD <i>E. huxleyi</i> (N)	35.27	0.260
LAD <i>P. lacunosa</i> (N)	62.82	0.460
Brunhes/Matuyama boundary	87.35	0.780
Jaramillo top	100.35	0.990
Jaramillo bottom	103.72	1.070
LAD <i>Gephyrocapsa</i> A/B (N)	111.46	1.230
Tie to 981	125.88	1.516
Tie to 981	127.75	1.545
Tie to 981	128.37	1.570
Tie to 981	129.95	1.595
Tie to 981	130.51	1.618
Tie to 981	131.15	1.630
Tie to 981	131.29	1.644
Tie to 981	132.49	1.672
Base of reflectance record	135.00	1.730

Note: FAD = first appearance datum, LAD = last appearance datum.